06/15/97

PPPL-3262, Reprint: September 1997, UC-420

Phenomenology of Major and Minor Disruptions in High β DT TFTR Plasma

S.Mirnov, I.Semenov

TRINITI, Moscow Reg., Russia

E. Fredrickson, R. Budny, Z. Chang, K. McGuire, H. Park, H. Takahashi,

S. Von Goeler, L. Zakharov, S. Zweben

Princeton University, Plasma Physics Laboratory, Princeton, NJ 08543, USA

ABSTRACT

This work presents the Magnetic probe data, Electron Cyclotron Emission (ECE), $\alpha-$particle losses, and Neutron flux data measured during the disruptive instability in high β TFTR plasmas. It is shown that the major disruptions in high β regimes go through several phases. The first phase is the fast (150-250 μsec) minor disruption (pre disruption) causing a drop of the central temperature (and possibly, density). In this phase a powerful central m=1/n=1 mode initiates the sequential development of m=4/n=1, 3/1, 2/1, 3/2 peripheral modes which lead to a 3/1 locked mode . The second phase is the slow thermal quench (2 ms) in the presence of a locked mode. The third phase is a fast positive current spike

(5-10% increase in Ip in less then 0.5 ms) and finally the current quench occurs with a loss of 2.5 MA in 5 ms.

1. INTRODUCTION

In this article we use the following definitions:

Minor disruption (or predisruption) is the growth of coupled edge and central MHD activity leading to a partial thermal quench, which can trigger fast growth of peripheral modes.

The Major disruption is a sequential development of MHD-activity beginning with the minor disruption and proceedings through the positive current spike and current quench.

Primary mode - is the tearing or kink mode which has positive or close to 0 positive growth. The behavior of this mode depends on (in general) global plasma parameters such as shear, presure profile, e.a. This mode determines the perturbation structure (the set of harmonic in toroidal geometry) over the plasma colomn.

Secondary mode - is the tearing or kink mode which has negative growth or close to 0 negative growth. The behavior of this mode depends on amplitude and phase of the primary mode.

It is known that the larger the tokamak dimensions, the more dangerous are the consequences of the disruptive instability. For large, ITER scale tokamaks the consequences of the disruption can be very serious. This situation motivates the study of the disruptive instability, especially in high β, high density, high current discharges. An example of a strong disruptive instability is TFTR DT shot #76778 in which a plasma

current of 2.5 MA and 9 MW of DT fusion power dropped to zero within 5 ms **[1].**

Two similar TFTR DT shots #76778 and #76773, (hereinafter referred to as #78 and #73) were compared in order to distinguish the main cause of the major disruption. In the case of #78 a major disruption occurred and in #73 only a minor disruption took place. The main subjects of this analysis are the poloidal magnetic field fluctuations, ECE-radiation, neutron radiation, α-particle losses and plasma density fluctuations. **Fig. 1a.b** shows the position of these diagnostics relative to the toroidal and poloidal cross section.

Fig. 2a, b show the signals of plasma current, magnetic fluctuations, α–particle losses at 270^0 (90^0 below the midplane in the ion grad B drift direction [1]), neutron and ECE emission from the central plasma region for shots #78 and #73. The first clear difference is the quasi stationary Bp oscillations before the minor disruption (phase "0") in the case #78, while the minor disruption #73 occurs with a much weaker precursor up to the time of the minor disruption. Both cases have fast growing ($\tau \cong 50$ μsec) MHD-activity with much the same amplitude. The second small difference lies in the amplitudes of α-losses and neutron emission. The central neutron emission drops 20% and 30% in the #73 and #78 cases respectively.

At first glance we could say these minor disruptions are the same, but after 2 msec #78 passes into a major disruption (Phases III, IV), while the magnetic activity in case #73 decreases and the discharge continues with degraded performance. It seems as though in both cases the magnetic activity in the center qualitatively has the same behavior. The difference

between these two minor disruptions is in the appearance of the locked mode in the case of #78.

2. MINOR DISRUPTION

Fig. 3a,b show the signals of plasma current, magnetic fluctuations, α–particle losses and neutron emission on an expanded time scale during the minor disruption for **shots #78** and **#73**

The experimental methodsused to analysed the data are briefly described in the next section.

2.1. Analysis of the external magnetic perturbations.

The newly developed method of magnetic perturbations visualization was applied for analysis of the discret experimental data array [2]. Magnetic perturbations are measured by toroidal and poloidal arrays of B_Θ probes (coils), which are located at various toroidal and poloidal positions. The main poloidal array has 15 coils and a toroidal array has 7 coils. To obtain a continuous screen picture we need to have a continuous function along the array's direction. The interpolation and smoothing was done by fitting the data with Lagrange or Chebyshev polynomials and then Fourier transforming to obtain a 180 point uniform grid. With this approximation, we have a continuous perturbation functions in the poloidal and toroidal directions. These functions are then used to control the brightness or color modulation of the display screen. Thus, it is possible to have a complete visual picture of the time dependent poloidal or toroidal structure of the perturbation behavior.

An example of this technique for poloidal perturbations is shown in **Figs. 4a, b** (top pictures), where brightness corresponds to the positive perturbations, dark to negative **[2].** These figures show a visual picture of the surface magnetic fluctuations before, during, and after the minor disruptions (phase 0, phase I and phase II) of shots #73 and #78. They cover the poloidal angles Θ from 0^0 to 360^0 (180^0 is the outer midplane of the plasma column). Middle and bottom plots show the toroidal and poloidal mode harmonics during the minor disruption.

As we can see from **Figs. 3a, b**, in both shots the rapid magnetic burst (phase Ia**, Fig. 3**) has the m=4/n=1 helical structure, which approximately corresponds to q(a)=4 near the plasma boundary. At the end of the phase Ia the fast m=4/n=1 burst in #78 explodes (Δt=3-5 μsec) into m=3/n=1 and m=2/n=1 (m=2/n=2) (Phase Ib, Fig. 4). (In the case #73 the fast m=4/n=1 changes into m=2/n=1, m=3/n=1). This abrupt change of the external MHD and the burst of α-particle losses may be the result of the inner plasma MHD activity near q=3, q=2 and q=3/2 and is a critical point of the minor disruption. It is desirably to understand the reason for this behavior. The analysis of the neutron and ECE emission behavior can give important information about the disruption development inside plasma.

2.2 Analysis of the central neutron emission

The neutron measurements **(Fig. 1b) [3]** provide (the most direct) information about internal processes in the hot DT plasma. A simple analysis, which was applied earlier for soft X-ray signals **[4]** allows us to separate odd and even modes near the plasma center. For two axially

symmetrical channels the difference of the signals will be proportional to the amplitude of the odd modes m=1, m=3 or to the displacement of the plasma core. The sum of these signals gives us information about the amplitude of the even modes m=0, m=2…. In shots #73 and #78 we have 7 chordal signals of the neutron emission (R=1.94, 2.23, 2.47, 2.47, 2.68, 3.00, 3.16 m, sampling time of 25 μsec). The poor signal/noise ratio in the outer channels allows us to use only the two central channels (R=2.68 m, close to the center of the plasma and 2.47 m, a little inside). **Fig. 5** shows the odd neutron signals and Bp magnetic probe signal **(shot #73**). It is easily seen that the internal odd neutron perturbation begins earlier than the rapid growth of the external magnetic m=4 perturbation. Also the odd signal correlates with the plasma density behavior in the center. The last signals are very similar but have opposite phase shift, because the neutron and n_e (MIRI) measurements have almost a 180^0 separation in toroidal positions. The different phase means that the perturbation is not a displacement of the plasma column, but probably is a result of perturbations with an **m=1/n=1** helical structure.

2.3 Analysis of the ECE emission

Analysis of the ECE information before and during the disruption gives very important information for understanding the dynamics of the disruption. Unfortunately, as it was determined earlier **[5]**, nonthermal emission appears during the disruption. It presents a severe problem for interpretation of the experimental results. However, we can use the ECE data from before the disruption.

ECE measurements were made by two grating polychromators (GPC1 and GPC2) separated by 126 degrees in the toroidal direction **[6]**. Evolution of the electron temperature profiles is shown in **Fig. 6a, b**, where segments **a-f** correspond to the time points indicated in **Fig 3a, b and Fig. 4a, b**. **Fig. 7** shows the electron temperature fluctuation $\Delta Te(t)$ at different plasma radii before the minor thermal quench (time interval 3.9221 -3.92236 sec case #73). Using the ECE measurements it is possible to estimate the relative displacement of the plasma and make a conclusion about the perturbation structure. Actually, if axially symmetric plasma regions have the temperature oscillations in phase, then the corresponding helical perturbations $\zeta(r)$ must be even (m=0,2,4...); in the opposite case the perturbations have odd structure (m=1,3..). Roughly, near the plasma center, we can separate odd and even perturbations subtracting or summing axisymmetrical $\Delta Te(t)$ traces. **Fig. 7** (bottom plot) shows that the perturbation in the plasma center begins as an odd mode, the even mode appears later at t=3.9223 sec and terminates at the minor thermal quench. The phase analysis of ECE, Ne, and Neutron fluctuations around the torus shows that the odd mode has m=1/n=1 helical structure. Right before the minor disruption it suddenly increases amplitude. The even mode (m=0) is the symmetrical cooling of the plasma center which follows by the m=1/n=1 disintegration. Following the symmetrical central cooling (m=0), the "MHD explosion" of perturbations near q(r)=2 and q(r)=3 starts 15-20 μsec later. In this moment the mode m=4/n=1 disappears and m=2 and m=3 harmonics appear in magnetic probe signals **(Fig. 4a, b)**. This can be interpreted as growth and, probably, reconnection of magnetic islands from q=1.5 to q=3 **[7, 8, 9]**. Unfortunately this picture is not clear because the ECE emission may have nonthermal component during this

process.**[10]** Nonthermal part of the ECE signal can be as a result of electron acceleration during magnetic island reconnection or, for example, connected with the interaction of fast ions and electrons with magnetic perturbations, and are driven by ion beams **[11]**. We have no quantitative model of this phenomenon. It should be point out that the appearance of nonthermal electrons is coincide in time and place with the probable position of q(r)=1.5-3 magnetic islands (Fig. 6a, b, frames d and e).

2.4 Event sequence during minor disruption

The most visible feature of minor disruption (in both cases #73 and #78) is the dBp/dt burst of external MHD activity (m=4/n=1), which can develops in the presence of slowly rising external precursor (m=4/n=1, #78) or without one (#73). In both cases the behavior of the neutron emission (Fig. 2 - 4 a, b) shows the fast explosive increase of m=1/n=1 in the center just before the burst of the external m=4/n=1 **[12].** The m=4/n=1 burst is clear visible in case #73. In #78 it is masked by preliminary m=4/n=1 activity. Internal development of m=1/n=1 (Fig. 7 t=3.92232 s) is finished by the Te(r) flattening near the center (m=0), which is similar to conventional sawtooth crash **[13].** The start of the m=2, m=3 harmonics (dBp/dt signal), α-losses (Fig. 3a, b), and the start of non thermal electron cyclotron emission near q(r)=1.5,2,3 begins 15-20 μsec later and, probably, is connected with the growth and reconnection of

magnetic islands. What is the origin of this explosion? The basis of Te(r) flattening probably is the complete or partial magnetic reconnection inside q(r)=1 as it happens in a sawtooth crash. During this process the current profile j(r) in the center, probably, has partial or complete flattening (li decreasing). It causes a decrease of the magnetic shear which usually is the main destabilizing factor for resonant MHD perturbations. (This is, for example, the explanation of the major disruption in small low-β tokamaks **[12]**). Additional destabilizing factor - ballooning modes, in high β plasmas appears in connection with high pressure gradient, . As it was published earlier **[14]** this instability in the form of 30 -50 kHz oscillations appears in high β TFTR plasma in the presence of m=1/n=1 activity. Fig. 3a, b shows typical burst of the ballooning modes (t= 3.9223 s). Obviously the amplitude of ballooning modes increases sharply when the m=1/n=1 amplitude grows. Maybe these modes leads to m=1/n=1 disintegration (m=0 development), and also can effect the internal m>1 modes destabilization.

Thus both minor disruptions in #73 and #78 have the same chain of events:

- fast (explosive) nonlinear m=1/n=1 development
  and subsequent ballooning modes excitation;
- m=4/n=1 external activity burst;
- burst of the m=0 in the center;
- destabilization of internal modes m>1;
- explosive cooling of the plasma column through the electron channel.

2.5 Possible long precursors of high beta disruptions

Fig 8a, b shows fluctuations of the electron temperature near the plasma center (R= 2.37 - 3.27 m) and magnetic perturbations at the edge of the plasma for 2 ms time interval before minor disruption for cases #78 (a) and #73 (b). In case of minor disruption the precursor should be distinguished as primary , which behavior depends on the plasma paramiters such as shear, presure profile, e.a. This precursor determins the predisruption process and secondary, which behavior depends on amplitude and phase of the primary mode.

Probably such a secondary precursors of the minor disruption in case #78 are slowly increase magnetic oscillations near the edge of the plasma, which are practically absent in the case #73. However both disruptions have a lot of common features, that we should expect may have the same origin and the same primary precursor.

It seems like that such a primary precursor can be T_e perturbations inside the plasma (Fig. 8a, b R=2.85 -3.00m, q=1-1.5) which can exists long before the minor disruption. They are localized near the maximum pressure gradient at the low Bt side, this is typical for ballooning modes. Phase analysis (GPC1, GPC2, Fig. 1) shows - for shot #78, that 1-2 ms before the minor disruption the perturbations have a helical structure, which is measured to be n=3 and even m (most probably m=4/n=3 **[10]**) In case #73 the perturbations has structure n=1 and odd m (m=1/n=1). It should be pointed out that n>1 perturbations have also been observed in high beta discharges in other tokamaks [9]. However it should be emphasized, that sometimes observable magnetic perturbations are absent before disruption. This is the main reason, why these magnetic modes can

not be primary the precursors. Maybe , they are the results of some pressure driven or neoclassical tearing mode instabilities **[15]**.

As we can see in the case of #78 (Fig. 9) the external and internal oscillations have independent behavior long before the disruption, their phases and frequencies are different (f=13 kHz for external and f=7-9 kHz for internal).

However, about 2ms before the disruption the frequency of the external mode m=4/n=1 gradually decreases to 9 kHz. When the external and internal frequencies becomes equal (Fig. 9 t=3.9508 s) there is a sudden phase jump of internal oscillations and they transform into m=1/n=1. From this moment the internal and external perturbations are strongly coupled in phase and amplitude. At the maximum amplidude of the m=1/n=1 a high frequency "ballooning" mode **[14]** appears and finally (Fig. 3a) the minor disruption develops in the above mentioned scheme: m=1/n=1 explosion, Te(r) flattening (m=0) and "MHD explosion" of m>1 perturbations across the entire plasma column.

So along this pathway to minor disruption all internal independent oscillations becomes strongly coupled with external m=4/n=1 MHD-activity **(Fig. 8b, Fig. 9).** The most probable reason for this coupling can be the loss of rotation velocity shear, that is, the transition of the plasma column into toroidal (rigit body) rotation. The experimentally observed frequency equalization of all modes can be the indicator of this transition (n=1) **[16]**. The loss of relative rotation of the regions with different q(r) gives a possibility for center - boundary phase resonance of different perturbations which looks like an increasing of the sensitivity of the plasma center to boundary perturbations, and conversely. Thus, the loss of

rotation shear makes it easier for the reconnection of magnetic islands with different helicity and, as a result, the magnetic stochasticity appears.

We can suppose that the loss of velocity rotation shear was the primary precursor of disruption in #78. In the case of # 73, weak external activity before disruption did not permit us to check the time evolution of the plasma rotation. We can say only that far from the disruption (3.9210 - 3.9215 sec, **Fig 8b)** the frequencies of central and boundary oscillations are different.

The disruption begins really at t=3.92218 s **(Fig. 3b , Fig. 5)** as sudden explosive growth of m=1/n=1 and development of the "ballooning" mode in the center. The explosion of the external mode **(Fig. 3b, Fig. 5)**, appears to be a consequence of this event.

However, 180 μs before the main m=1/n=1 explosion (t=3.9220 s), we can see (R=2.998-2.92 m ,Fig. 8b, Fig. 3b, GPC1) the start of high frequency (30 KHz) "ballooning"-like oscillations and, as a result, some Te(r) flattening in this region. The analysis shows the appearance of additional external (Bp , m=4/n=1) and internal, (probably m=1/n=1) perturbations 100 μs later than the start of "ballooning". The main m=1/n=1 mode starts in the center approximately 160 μs later than the "ballooning" mode. Simultaneously the preliminary Bp perturbations breaks up and a new m=4/n=1 burst starts in phase with m=1/n=1 **(Fig. 2b).** We believe this case shows us the center - boundary resonance in detail, which is preceded by minor disruption. We should not exclude the possibility that the origin of this resonance can be the loss of shear velocity, like in the case #78.

Thus, we do not see clearly one primary precursor of the minor disruption in shots #78 and #73 but, we suppose that the loss of rotation shear and, as a result the center-bondary resonance is the such precursor.

In high beta the "ballooning" or "ballooning"-like modes probably are the results of pressure driven or neoclassical tearing mode instabilities and play some important role in m=1/n=1 destabilization.

3. TRANSITION INTO MAJOR DISRUPTION

After the minor disruption the Te(r) flattens in the core and a slowing of the plasma rotation occur (See **Fig 4a, b, Fig. 6a , b)**. In the case of #78, a locked mode with m=3 appears. **Fig. 10** shows the picture of the surface Bp(θ,t) fluctuations (dBp/dt probes signals were numerically integrated) during the minor disruption and formation of the m=3 locked mode. The development of the locked modes probably causes the cooling of electron and ion plasma components. Measurements of Te(r) in this phase **(Fig. 6b, a)** show the flattening in the center after the minor disruption and cooling of peripheral plasma regions before the major disruption **[17]**.

Unfortunately we have no reliable information (other than neutron emission) for the time between minor and major disruptions in case of #78 (the magnetic probe signals are saturated and the ECE and density interferometer signals have questionable behavior, see **Fig. 2a**). Basically, the time behavior of the ECE, α-particle losses, and neutron emission show that this process is not simple plasma cooling. It looks like a chain of sequential internal MHD explosions.

The traces of the neutron collimator are shown in **Fig. 11.** The plasma thermal quench goes through two stages, slow and fast. During the phase II the neutron rate monotonically decreases from 3.9516-3.9528 sec after which the fast phase III begins. At this moment MHD activity, which

leads to the current quench, appears in the outer region of the plasma on the neutron channels viewing from position at R=194 cm, R=208 cm and R=316 cm. The neutron perturbation begins near the radius R=208 cm and after the initial decrease there occurs an increase of neutrons, which might be caused by the transport of hot ions from the plasma core. The neutron intensity also may increase in the outer channel (R=316 cm), however this is not completely clear because at this time there may be an inward shift of the plasma column. The radial position of these outer channels is in the region q(r)=2-3. So far no instabilities have been identified with certainty that explain the observed neutron behavior. As a result we can suppose that the general cooling, probable j(r) flattening, and decrease of the magnetic shear in the plasma center (Phase III) could create the condition for helical mode development (tearing or ideal kink). As a non-linear form of ideal kink can be the appearance of the Kadomtsev-Pogutse vacuum bubbles **[18]** which can lead to fast li drop, global stochastisity, and a positive spike of plasma current generation, that was obtained experimentally. Plasma-wall interaction attends this process and could possibly cause the cooling of the plasma center by impurities from the wall and is followed by the current quench (Phase IV).

Finally, we should remark that in the shot #81919 **[17]** (this shot has the similar conditions, as #76778) was shown that just before positive current spike generation (end of the Phase III) Te(r) profiles have a very broad, cold pedestal which can be the result of a locked mode **[19]**, or impurity cooling and very narrow peaked Te(r) profile in the q(r)~1 region.

The positive current generation precedes very fast (100 μs) the T_e profile erosion as the result of m=1/n=1 perturbation development. Similar fast precursors before major disruption were observed earlier **[12, 16]** in small and large **[19]** tokamaks.

4. CONCLUSIONS

The analysis of internal and external MHD-activity in TFTR shots #73 and #78 on the basis of magnetic, neutrons and ECE measurements shows:

1. The major disruption in high β TFTR plasma **goes through 4 main phases**:

Phase I. A fast (150-250 μsec) minor disruption with flattening of the temperature, and possibly also the density, in the plasma core.

Phase II. A slow thermal quench (2 ms) with progressive cooling of the center in the presence of a visible locked mode.

Phase III. Fast plasma current spike (≅10% Ip, t≅100-200 μs)

Phase IV Finally, the current quench (#78 2.5 MA/5 ms).

2. The minor disruption seems to be the key event in this chain.

3. The minor disruption can exist without causing a major disruption, although it is accompanied by strong perturbations in the plasma center.

4. The magnetic signals show the minor disruption can develop with a long magnetic precursor oscillation, or can be without one. In both cases the magnetic activity increases strongly just before the minor disruption.

The first magnetic burst (Phase **Ia**) has a helical structure with m close to q(a), but after 20-50 μsec from the start, this structure breaks and there is a fast (5 μsec) transformation into a secondary burst (Phase **Ib**) with m=3/n=1 (3/2) or m=2/n=1 or both. At this time the first α-particle and non-thermal ECE bursts appear. This indicates that there are large perturbations in the plasma center. After this phase the MHD activity drops, and the plasma rotation decreases. Locked modes can develop at this time (Phase **Ic**).

5. The measurements of plasma density and neutron emission show the rapid grouth of odd perturbations in the center, probably m=1/n=1, which precede the first magnetic burst. The development of these modes is interrupted by the m=0 perturbation , which proceeds (10-20 μs) the secondary magnetic burst (m=3/n=2) and m=0 causes the flattening of the neutron emission.

6. The ECE (thermal part) measurements confirm qualitatively this sequence of events. Also, ECE shows two types of precursors. The first is a long precursor with low frequency (7-9 kHz, m=4/n=3, m=1/n=1) and the second one is high frequency (50-100 kHz, n>>1) and localized near q(r) =1-2. Both precursors have ballooning character and look like pressure gradient driven or neoclassical tearing modes. A high frequency mode accompanies the m=1/n=1 internal activity and maybe plays an important role in the sudden decrease in the amplitude of the m=1/n=1 structure.

7. The "MHD explosion" (m=2, m=3) which was followed by an internal precursor can be the result of magnetic shear loss during the central flattening or a result of direct magnetic stochastization in the q(r)>1 region that can be generated by "ballooning" modes **[14]**.

8. The high sensitivity of the central MHD modes to boundary modes, and boundary MHD modes to central ones, can be explained by the loss of velocity shear before minor disruption (equalization of rotational velocities at different magnetic surfaces and plasma column transition into toroidal (rigid body) rotation).

9. The ECE measurements indicate the appearance of non thermal electrons during the "MHD - explosion" (Phase Ib, Ic) near q(r) =2 and 3.

10. The transition period between minor and major disruptions is the gradual plasma cooling under the influence of locked modes and impurities.

Finally these experimental results suggest the following chain of events that lead to minor and major disruption in high β TFTR shots:

1. Plasma heating increases the pressure gradient in the plasma center.

2. Appearanece of plasma-center resonace (high sensitivity of the center to boundary perturbations, and the opposite)., for example, by transition into toroidal rigid body rotation (case #78).

3. The explosion of m=1/n=1 and high frequency "ballooning" modes.

4. Rapid growth of the boundary mode with m close to q(a) (for shots #76778, #76773 this is m=4) and the appearance of m=0 in the center (profile flattening).

5. The burst of the m=2/n=1 (3/2), m=3/n=1 external modes, burst of α-particle losses, and nonthermal electrons near q(r)=2 and 3.

6. The end of the minor disruption, the disappearance of dangerous gradients, and the decrease of plasma rotation, (sometimes locking).

7. Cooling of the plasma center. Collapse of T_e, n_e, and neutron emission. The positive current spike and current quench in a cold plasma.

ACKNOWLEDGMENTS

We thank J. D. Callen, H. Furth, E. J. Strait for fruitful discussions. We also thank K. Young and R. Hawryluk for their continued support of these studies. Finally we thank O. Semenov for help in visualization of the magnetic fluctuations.

REFERENCES

[1] M. Bell, et al. Conf. IAEA -15, report IAEA-CN-60/A-2-I-1 (1994).

[2] I. Semenov, et al. 22nd meeting of the European Physical Society, July 1995, Bournemouth UK, p114.

[3] Von Goeler, A.Roquemore, L.Johnson, M.Bitter, M.Diesso, E.Fredrikson, D.Long, and J.Strachan Submitted Rev. Sci. Instruments 1996.

[4] S. Mirnov, I. Semenov IAEA-6, 1977, v.1, p.291.

[5] E. Fredrickson, S. Batha, M. Bell ea. 15-IAEA Int. Conf., Seville, 1994 IAEA-CN-60/a-3-I-4.

[6] K. McGuire, H. Adler, P. Alling e.a. Physics of Plasmas, 2 (6), June 1995.

[7] L. Zakharov, Rus. Phys. Plasma, v.7, n.1, (1981), p.18.

[8] G. Bateman, MHD Instability, MIT Press 1979.

[9] H. Zohm e.a. Plasma Phys. and Controlled Fusion, v. 37, Suppl. 11a, Nov. 1995, A313, EPS-22 conf. Bournemouth, 1995.

[10] E. Fredrickson, K. McGuire, Z. Chang, M. Bell, R. Budney, C. Bush, J. Manickam, H. Mynick, R. Nazikian, and G. Taylor, Phys. Plasmas 2 (11), November 1995.

[11] T. Ohkawa, Nucl.Fus. 1970, V.10, N.2, p.185,

[12] S. Mirnov, I. Semenov -EPS-8, 1977, v. 1, p. 45

[13] S. Von Goeler EPS-7, 1975, v.II, p.71.

[14] W. Park, E. Fredrickson et. al., Phys. Rev. Lett. 75, n. 9, (1995), 1763.

[15] R. Carrera, R. D. Hazeltine and M. Kotscherenter, Phys. Fluid 29, 899 (1986)

[16] F. Karger et. al. IAEA-6, (1977), v. 1, p. 267.

[17] E. Fredrickson et. al., EPS-22, Bournemouth, (1995), v.3, p. 045.

[18] B. Kadomtsev, O. Pogutse , Sov. Phys JETP 38 (1974) 283.

[19] J. Wesson, R. Gill, et.al., Nucl. Fus. 26 (1989) 641

FIGURES CAPTIONS

Figure 1 The position of the measurement channels of the Electron Cyclotron Emission (ECE), Neutron Flux collimator (Neutrons), α-losses detector (Alfas) and Magnetic probes (Mirnov coils) in toroidal (a) and poloidal cross sections (b).

Figure 2 Behavior of the Ip-plasma current, -magnetic probe signals, α-losses, neutrons and ECE signals during minor and major disruption.

a) - shot # 76778 (major and minor disruption).

b) - shot #76773 (minor disruption).

Figure 3 Phases of the minor disruption:

Ia - rapid growth of the external $m \cong q(a)=4$ mode;

Ib - fast "explosive" transformation of m=4 into m=3 and m=2;

Ic - reconstruction and relaxation of the magnetic fluctuations.

The locked mode appears at the end of this phase.

a) shot #76778

b) shot #76773

Figure 4 The structure of the boundary magnetic fluctuations in a minor disruption shown in coordinates of poloidal angle and the time with dB_p/dt amplitude as a brightness. $\Theta=0$ corresponds the to internal midplane of the torus (upper

plot). The corresponding amplitudes of the toroidal and poloidal harmonics are shown as a function of time in the middle and bottom plots.

a) - shot #76778

b) - shot #76773

Figure 5 Comparison of the central odd mode, calculated from fluctuations of the neutrons with the plasma density fluctuations in the center of the plasma and external magnetic activity at the earlier phase of the minor disruption. Internal odd (m=1) mode probably starts first.

Figure 6 Profiles of the electron temperature during the minor disruption obtained by GPC1 (solid curve) and GPC2 (dashed). Profiles **a-f** correspond to the time points **a-f** of Figs. 3a,b, 4a,b, 7, 8. The comparison of these profiles shows the scale of influence for different MHD perturbations on the plasma column. **a**-n=3 perturbations before minor disruption, **b** - profile deformation as a result of ballooning mode development, **c** -influence of the fast m=1/n=1 internal mode, **d** - profile deformation as a consequence of the islands development in the region q=1-2, **e** - nonthermal emission from the stochastic islands region, **f**-(#73) Te profile in the relaxation stage of the minor disruption and (#78) during thermal quench in phase II of the major disruption.

a) - shot #76778

b) - shot #76773

Figure 7 Behavior (shaded regions) of the odd (most probably m=1) and even (m=0, m=2...) perturbations during the minor disruption (ECE - measurements)

Figure 8 $\Delta Te(R,t)$ fluctuations for several msec before minor disruption. Clear visible oscillations (R=292 cm) exist in central plasma regions near q=1-1.5 long before minor disruption. Observed oscillations evidently are an important feature of high β discharges.

a) - shot #76778

b) - shot #76773

Figure 9 Quasi stationary oscillations (n=3) appear at maximum grad P near the plasma center then rapidly change into m=1/n=1. This change is accompanied by strong coupling of the m=1 with higher m and is likely a real precursor of the disruption. Strong coupling m=1 and m>1 is an important feature that distinguish this phenomena from sawtooth oscillations.

Figure 10 Transformation of the boundary rotational m=4 mode into locked mode during the minor disruption shown in coordinates of poloidal angle and time with B_p/dt amplitude as a brightness. Θ=0 corresponds to the internal midplane of the torus. **(**Shot #76778. Probe data were numerically integrated).

Figure 11 Behavior of the neutron emission during the major disruption.

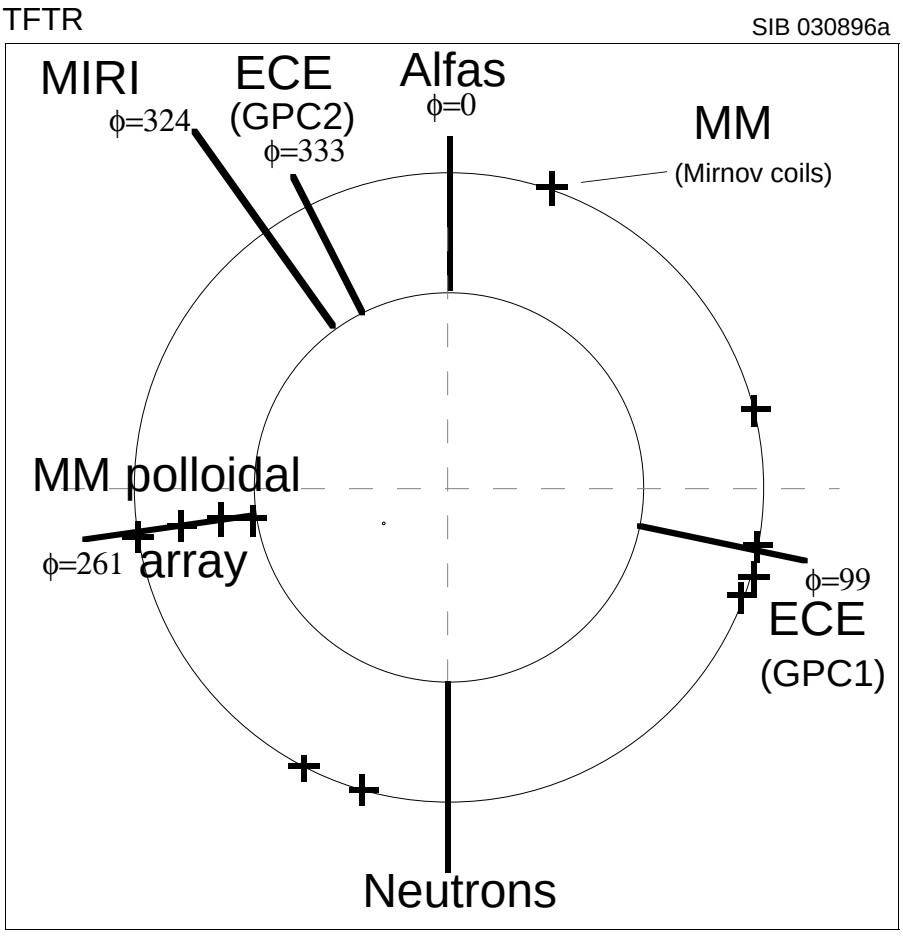
TFTR
SIB 030896a
MIRI
ϕ=324
ECE
(GPC2)
ϕ=333
Alfas
ϕ=0
MM
(Mirnov coils)
MM polloidal
array
ϕ=261
ϕ=99
ECE
(GPC1)
Neutrons

(a)

Figure 1a

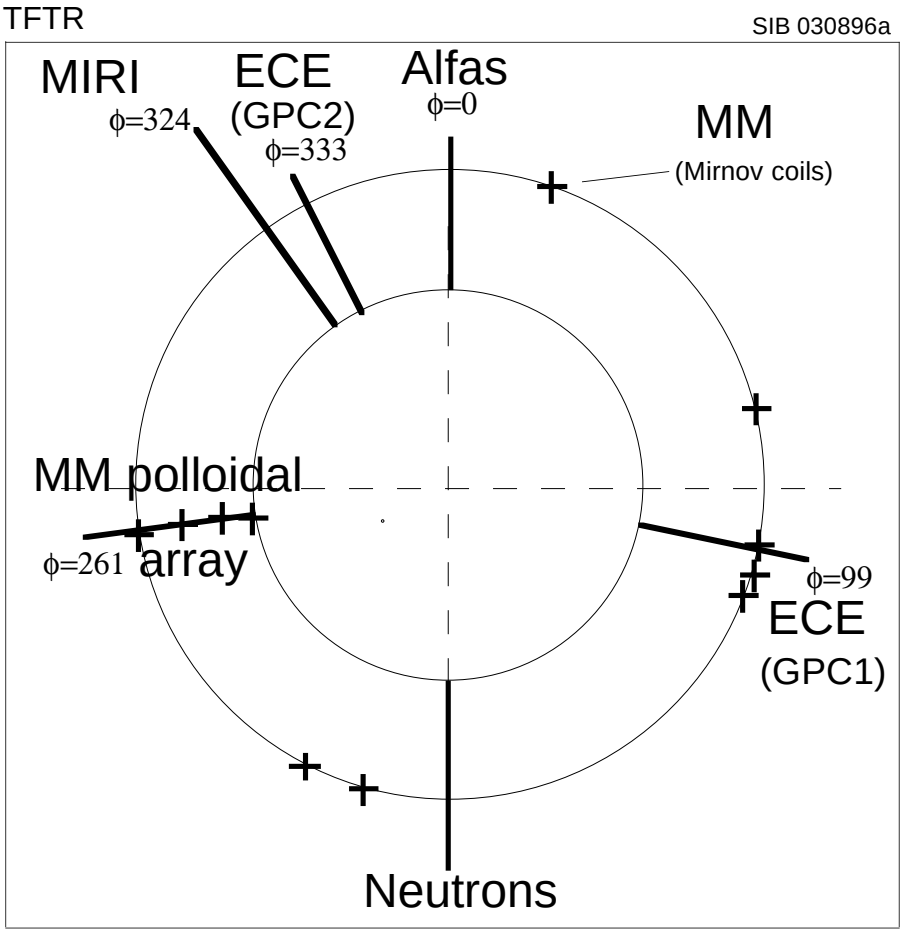
TFTR
SIB 030896a
MIRI
ϕ=324
ECE
(GPC2)
ϕ=333
Alfas
ϕ=0
MM
(Mirnov coils)
MM polloidal
array
ϕ=261
ϕ=99
ECE
(GPC1)
Neutrons

(a)

Figure 1a

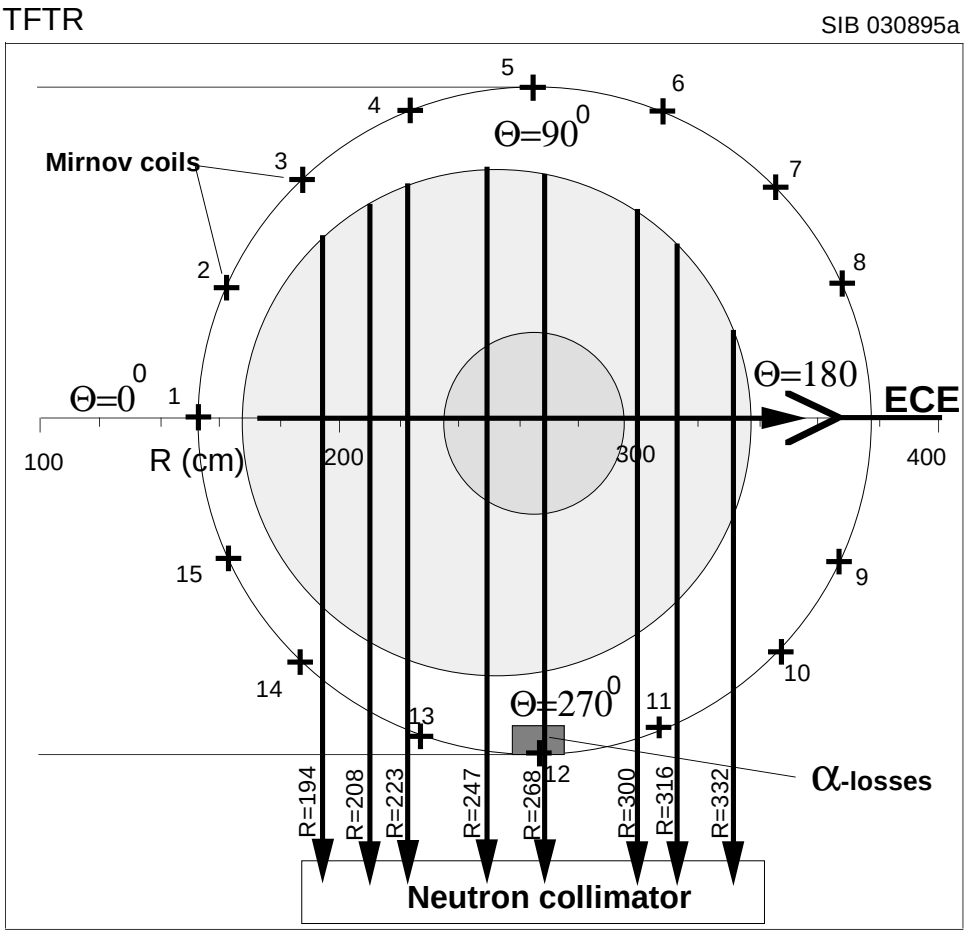
TFTR
SIB 030895a
Mirnov coils
Θ=90^0
Θ=0^0
Θ=180
ECE
Θ=270^0
R (cm)
100
200
300
400
α-losses
R=194
R=208
R=223
R=247
R=268
R=300
R=316
R=332
Neutron collimator

(b)

Figure 1b

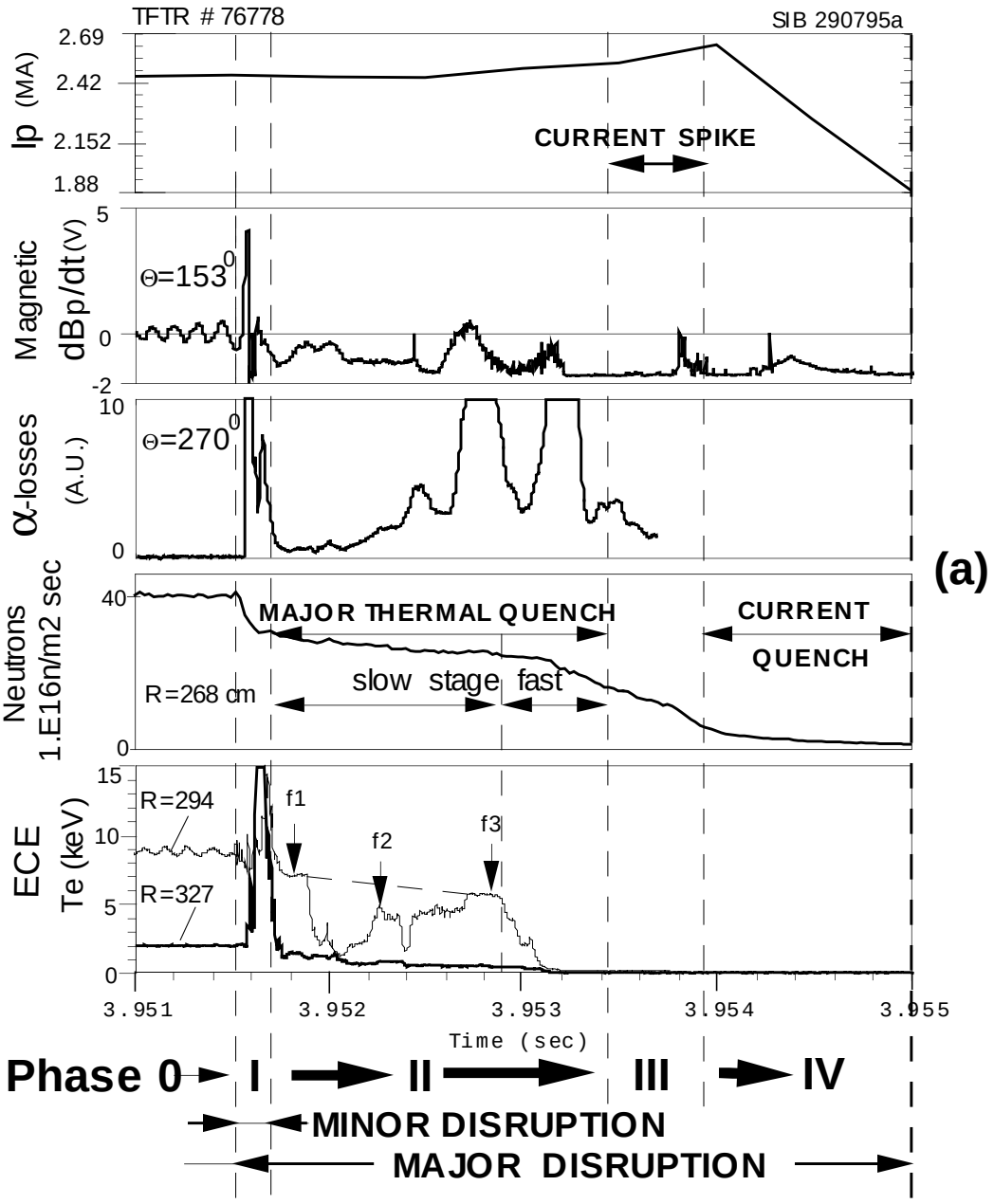
TFTR # 76778
SIB 290795a
Ip (MA)
2.69
2.42
2.152
1.88
CURRENT SPIKE
Magnetic dBp/dt(V)
Θ=153°
5
0
-2
α-losses (A.U.)
Θ=270°
10
0
(a)
Neutrons 1.E16n/m2 sec
40
MAJOR THERMAL QUENCH
CURRENT QUENCH
R=268 cm
slow stage fast
0
ECE Te (keV)
15
10
5
0
R=294
R=327
f1
f2
f3
3.951
3.952
3.953
3.954
3.955
Time (sec)
Phase 0
I
II
III
IV
MINOR DISRUPTION
MAJOR DISRUPTION

Figure 2a

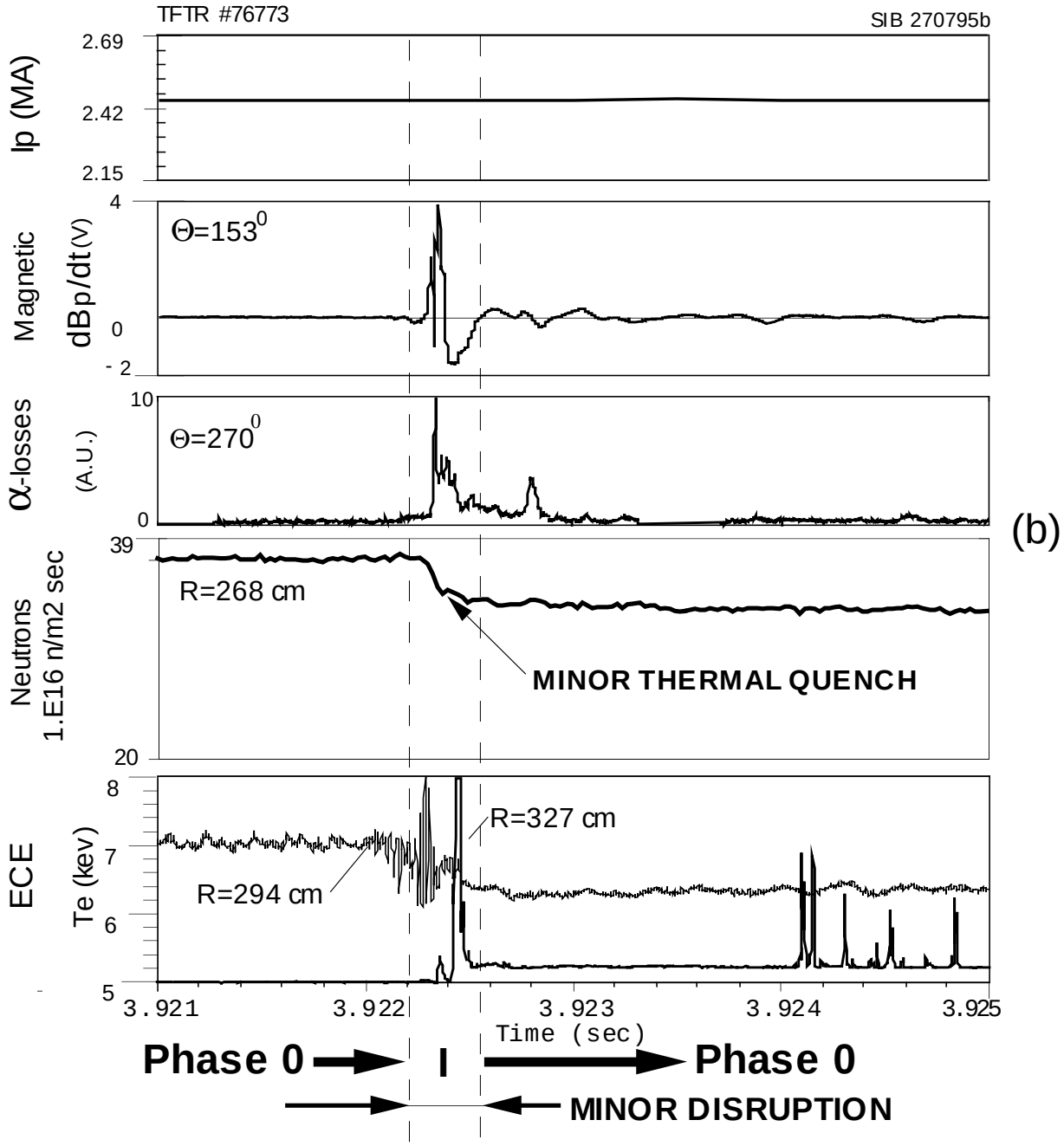
TFTR #76773
SIB 270795b
Ip (MA)
2.69
2.42
2.15
Magnetic dBp/dt(V)
4
0
- 2
Θ=153^0
α-losses (A.U.)
10
0
Θ=270^0
(b)
Neutrons 1.E16 n/m2 sec
39
20
R=268 cm
MINOR THERMAL QUENCH
ECE Te (kev)
8
7
6
5
R=294 cm
R=327 cm
3.921
3.922
3.923
3.924
3.925
Time (sec)
Phase 0
I
Phase 0
MINOR DISRUPTION

Figure 2b

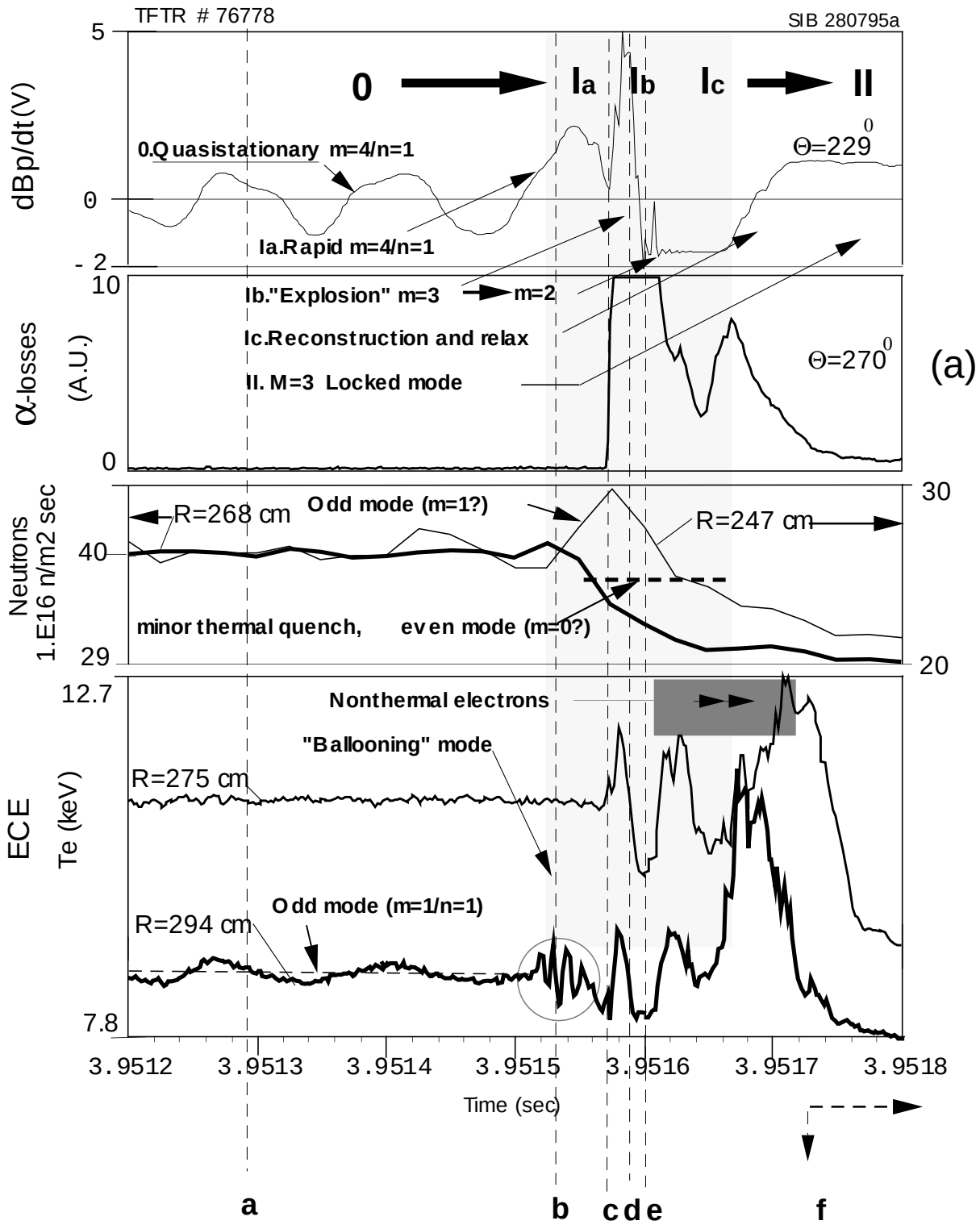
TFTR # 76778
SIB 280795a
dBp/dt(V)
0
Ia
Ib
Ic
II
0.Quasistationary m=4/n=1
Θ=229 0
Ia.Rapid m=4/n=1
Ib."Explosion" m=3
m=2
Ic.Reconstruction and relax
II. M=3 Locked mode
Θ=270 0
α-losses (A.U.)
(a)
Neutrons 1.E16 n/m2 sec
R=268 cm
Odd mode (m=1?)
R=247 cm
minor thermal quench,
even mode (m=0?)
Nonthermal electrons
"Ballooning" mode
R=275 cm
ECE Te (keV)
Odd mode (m=1/n=1)
R=294 cm
Time (sec)
a
b
c
d
e
f

Figure 3a

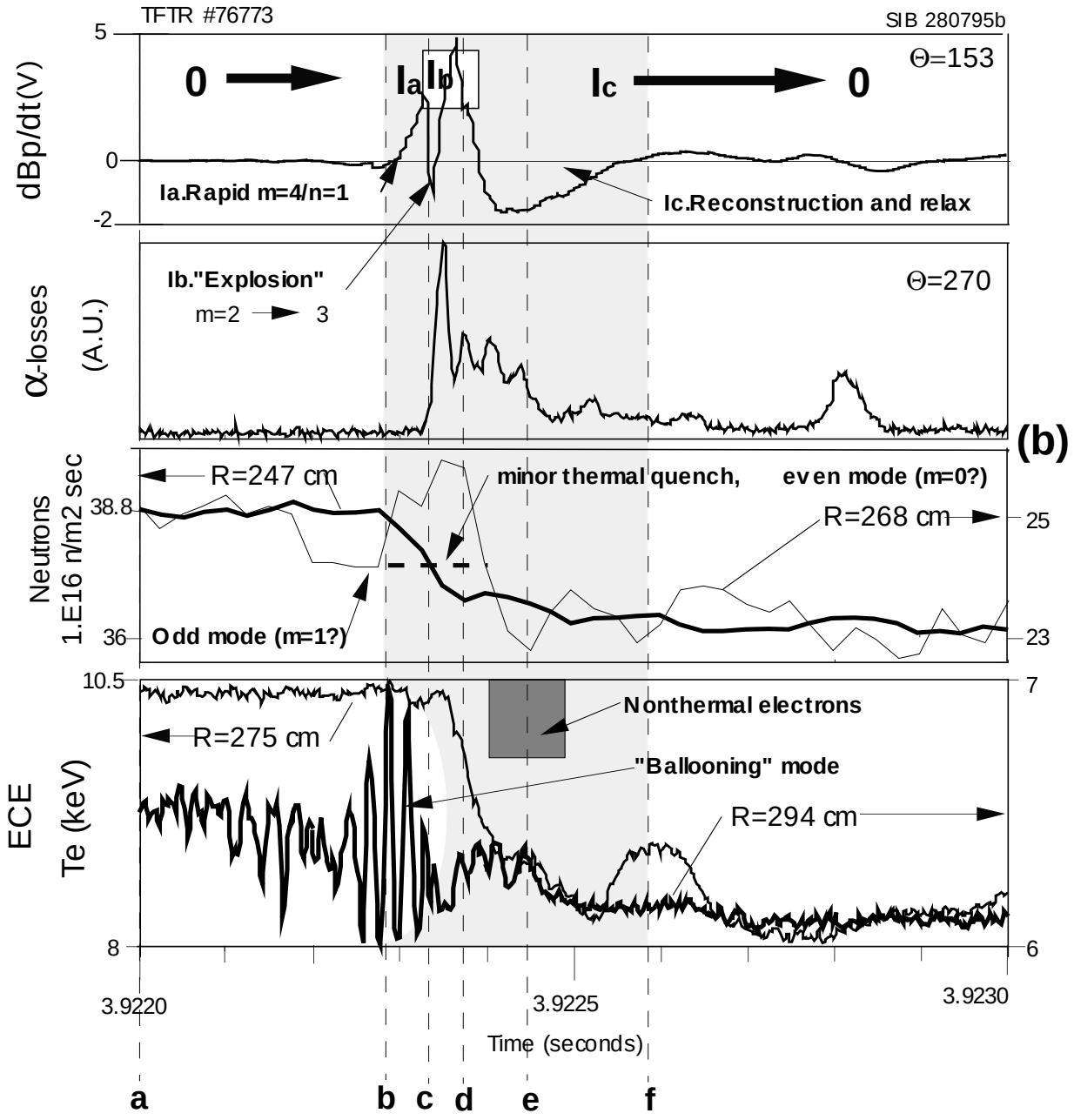
TFTR #76773
SIB 280795b
dBp/dt(V)
5
0
-2
0
Ia Ib
Ic
0
Θ=153
Ia.Rapid m=4/n=1
Ic.Reconstruction and relax
Ib."Explosion"
m=2 → 3
α-losses (A.U.)
Θ=270
(b)
Neutrons 1.E16 n/m2 sec
38.8
36
R=247 cm
minor thermal quench,
even mode (m=0?)
R=268 cm
25
23
Odd mode (m=1?)
ECE Te (keV)
10.5
8
7
6
R=275 cm
Nonthermal electrons
"Ballooning" mode
R=294 cm
3.9220
3.9225
3.9230
Time (seconds)
a
b
c
d
e
f

Figure 3b

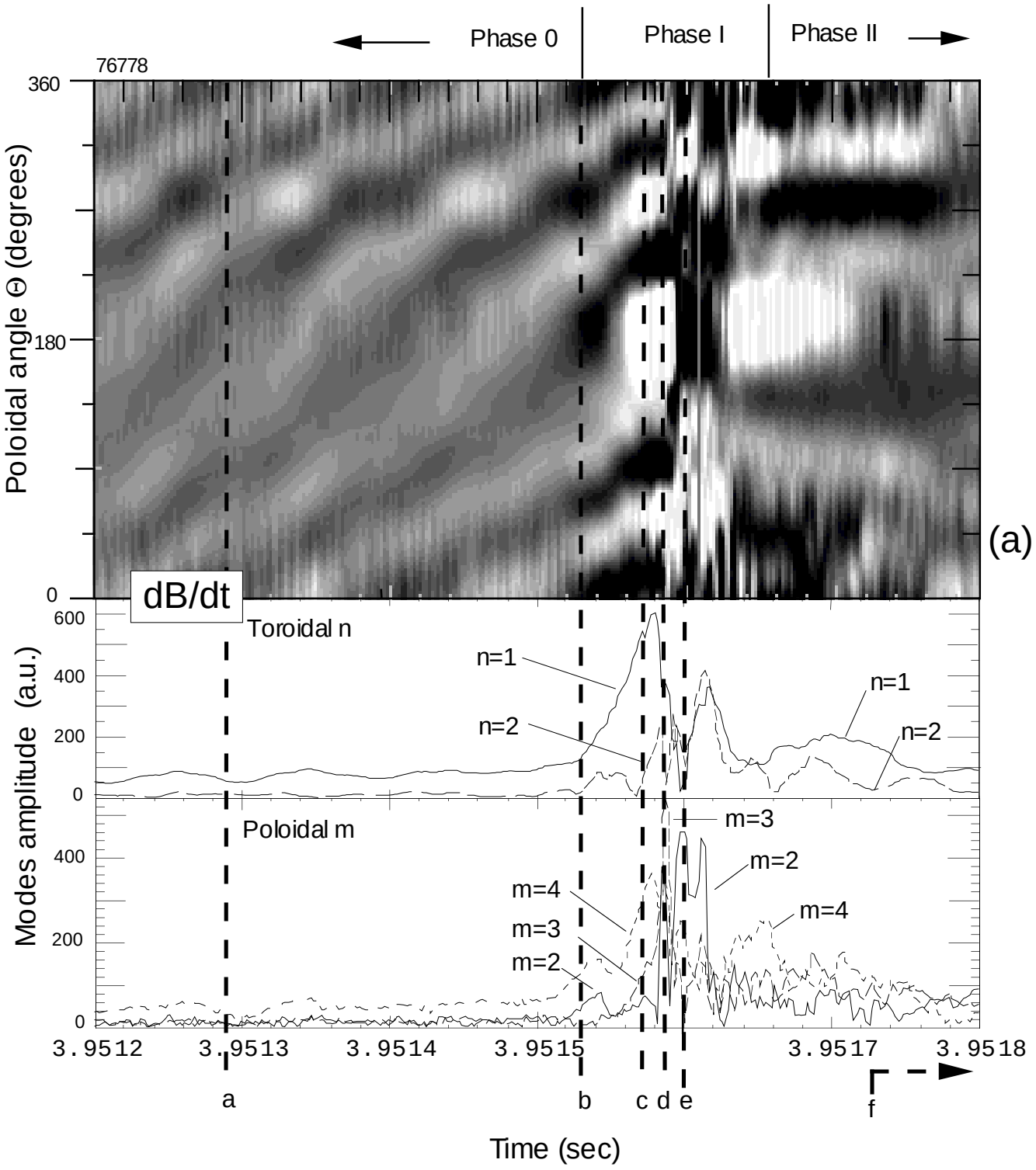
Phase 0
Phase I
Phase II
76778
360
180
0
Poloidal angle Θ (degrees)
(a)
dB/dt
Toroidal n
n=1
n=2
n=1
n=2
600
400
200
0
Modes amplitude (a.u.)
Poloidal m
m=3
m=2
m=4
m=4
m=3
m=2
400
200
0
3.9512
3.9513
3.9514
3.9515
3.9517
3.9518
a
b
c
d
e
f
Time (sec)

Figure 4a

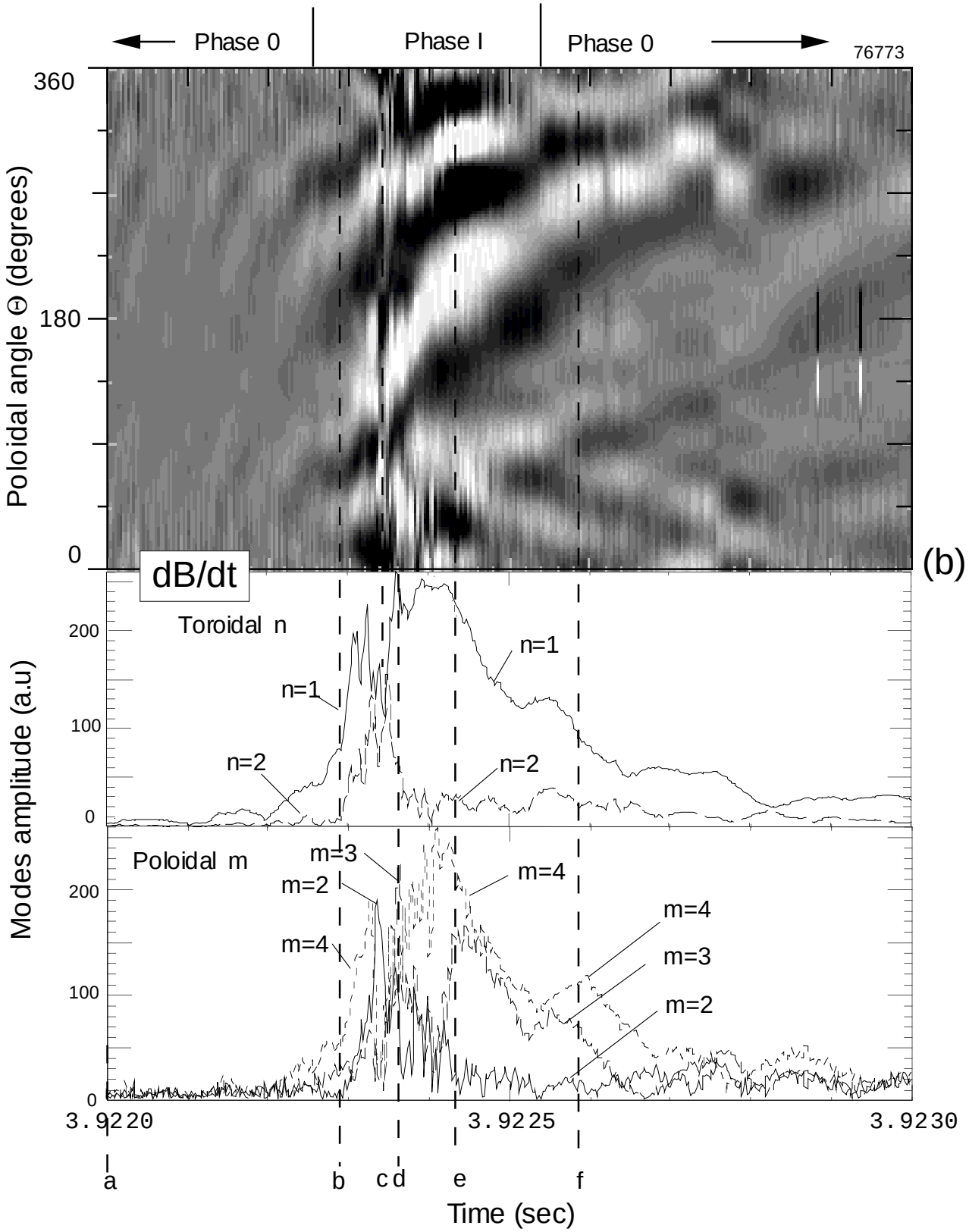
Phase 0
Phase I
Phase 0
76773
360
180
0
Poloidal angle Θ (degrees)
(b)
dB/dt
Toroidal n
n=1
n=1
n=2
n=2
200
100
0
Poloidal m
m=3
m=2
m=4
m=4
m=4
m=3
m=2
Modes amplitude (a.u)
3.9220
3.9225
3.9230
a
b
c
d
e
f
Time (sec)

Figure 4b

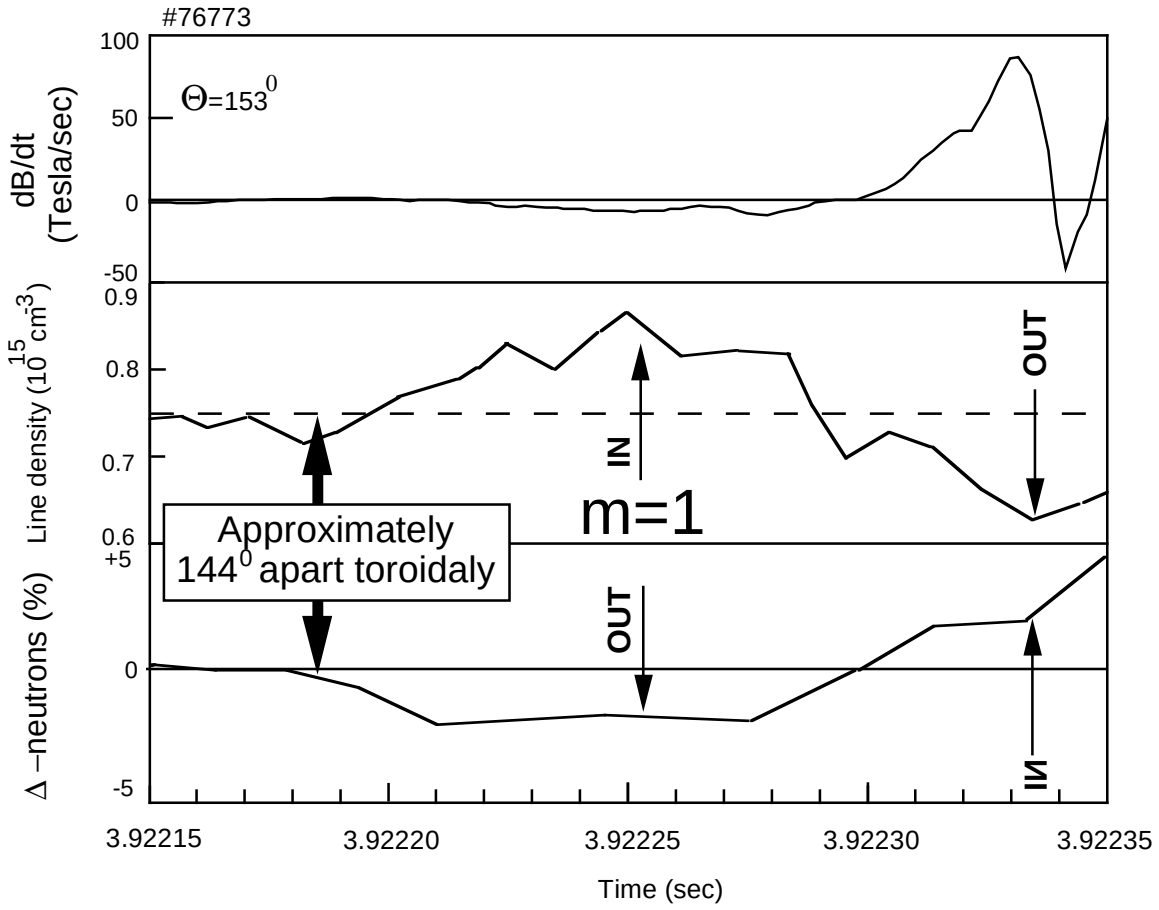
#76773
100
50
0
-50
dB/dt
(Tesla/sec)
Θ=153^0
0.9
0.8
0.7
0.6
Line density (10^15 cm^-3)
OUT
IN
m=1
Approximately
144^0 apart toroidaly
+5
0
-5
Δ –neutrons (%)
OUT
IN
3.92215
3.92220
3.92225
3.92230
3.92235
Time (sec)

Figure 5

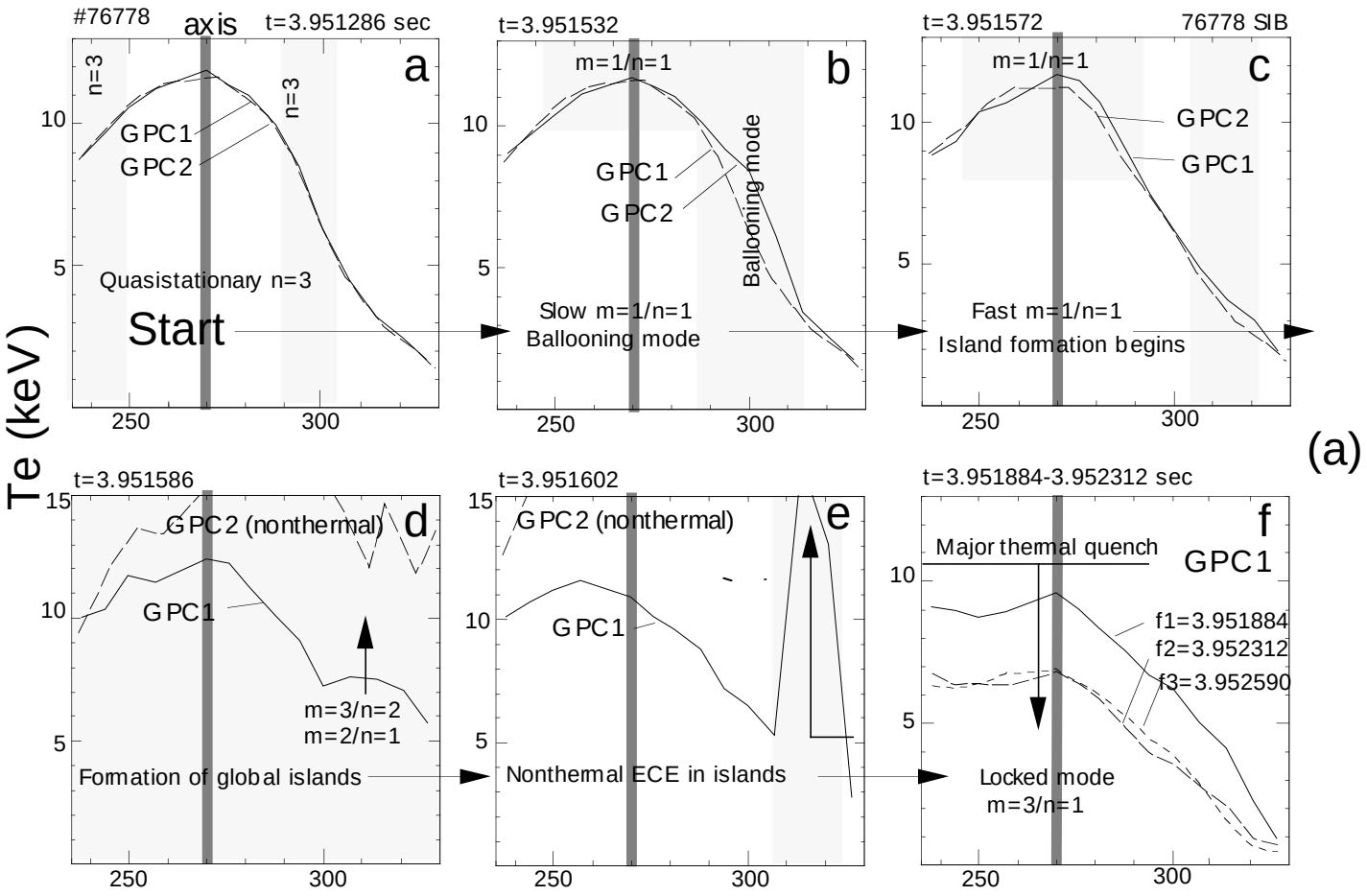
#76778
axis
t=3.951286 sec
a
n=3
n=3
GPC1
GPC2
Quasistationary n=3
Start
t=3.951532
m=1/n=1
b
GPC1
GPC2
Ballooning mode
Slow m=1/n=1
Ballooning mode
t=3.951572
76778 SIB
m=1/n=1
c
GPC2
GPC1
Fast m=1/n=1
Island formation begins
(a)
Te (keV)
t=3.951586
d
GPC2 (nonthermal)
GPC1
m=3/n=2
m=2/n=1
Formation of global islands
t=3.951602
e
GPC2 (nonthermal)
GPC1
Nonthermal ECE in islands
t=3.951884-3.952312 sec
f
Major thermal quench
GPC1
f1=3.951884
f2=3.952312
f3=3.952590
Locked mode
m=3/n=1
Major radius (cm)

Figure 6a

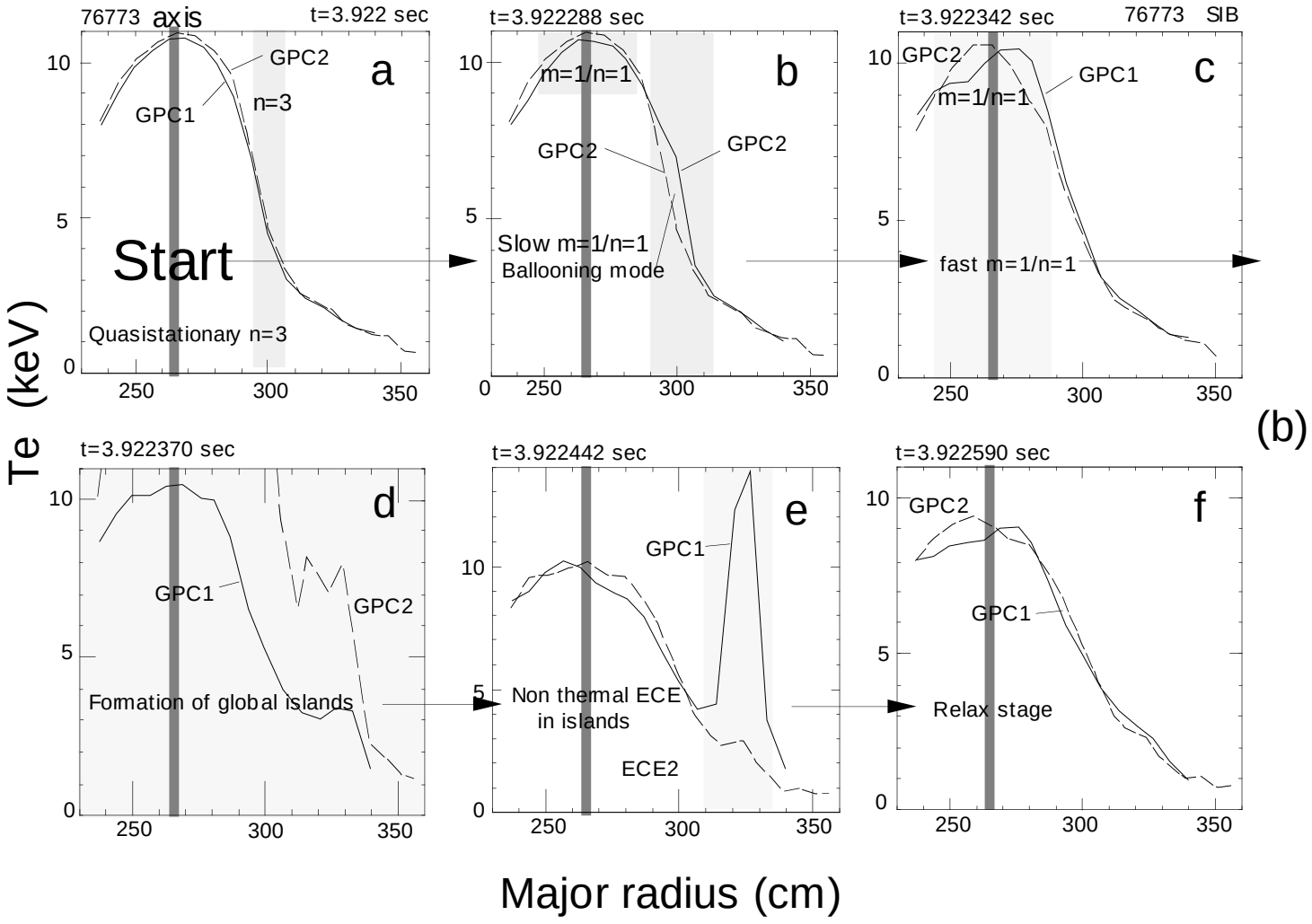
76773 axis
t=3.922 sec
a
GPC2
GPC1
n=3
Start
Quasistationary n=3
t=3.922288 sec
b
m=1/n=1
GPC2
GPC2
Slow m=1/n=1
Ballooning mode
t=3.922342 sec
76773 SIB
c
GPC2
GPC1
m=1/n=1
fast m=1/n=1
(b)
Te (keV)
t=3.922370 sec
d
GPC1
GPC2
Formation of global islands
t=3.922442 sec
e
GPC1
Non thermal ECE
in islands
ECE2
t=3.922590 sec
f
GPC2
GPC1
Relax stage
Major radius (cm)

Figure 6b

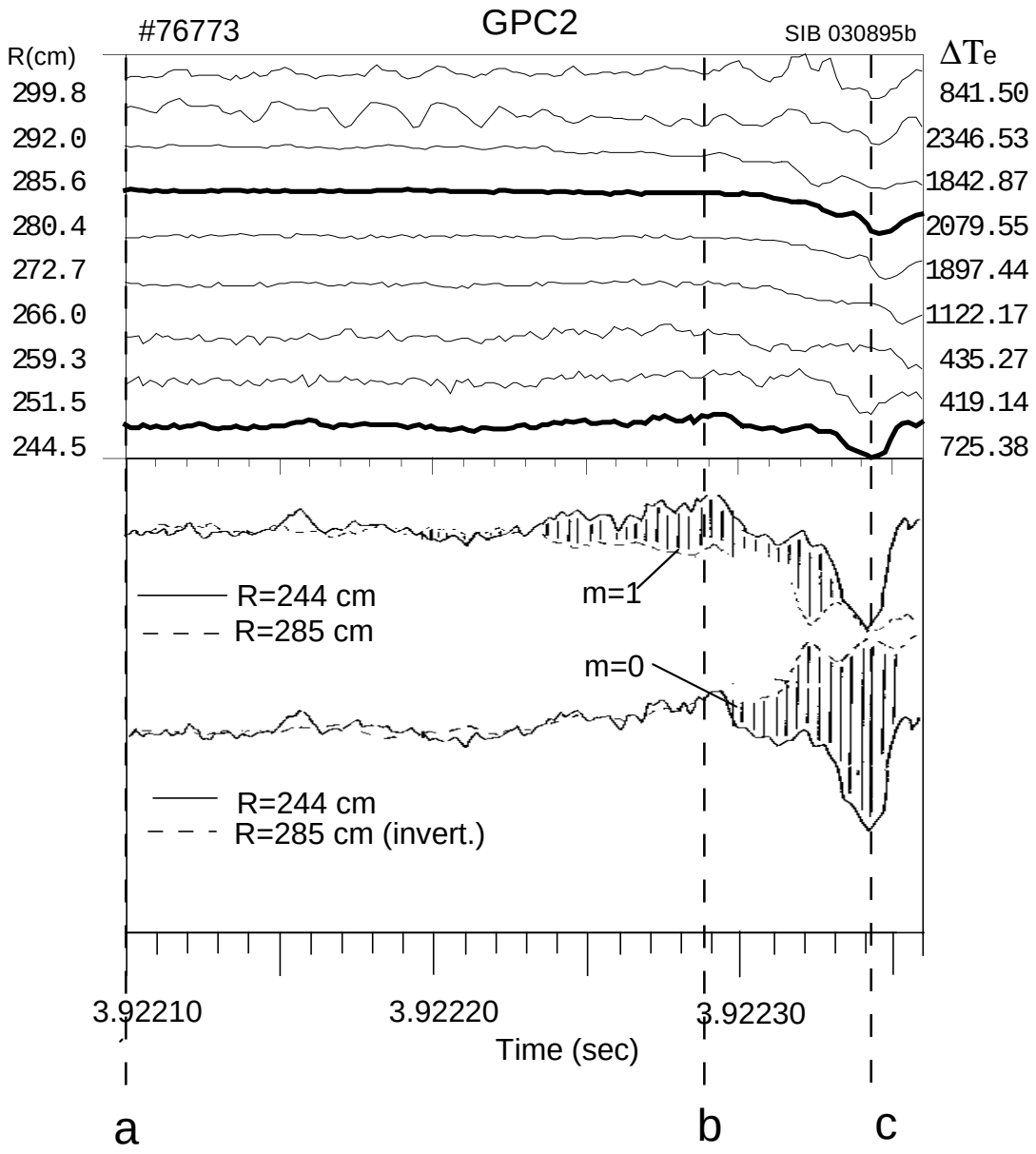
#76773
GPC2
SIB 030895b
R(cm)
299.8
292.0
285.6
280.4
272.7
266.0
259.3
251.5
244.5
ΔTe
841.50
2346.53
1842.87
2079.55
1897.44
1122.17
435.27
419.14
725.38
R=244 cm
R=285 cm
m=1
m=0
R=244 cm
R=285 cm (invert.)
3.92210
3.92220
3.92230
Time (sec)
a
b
c

Figure 7

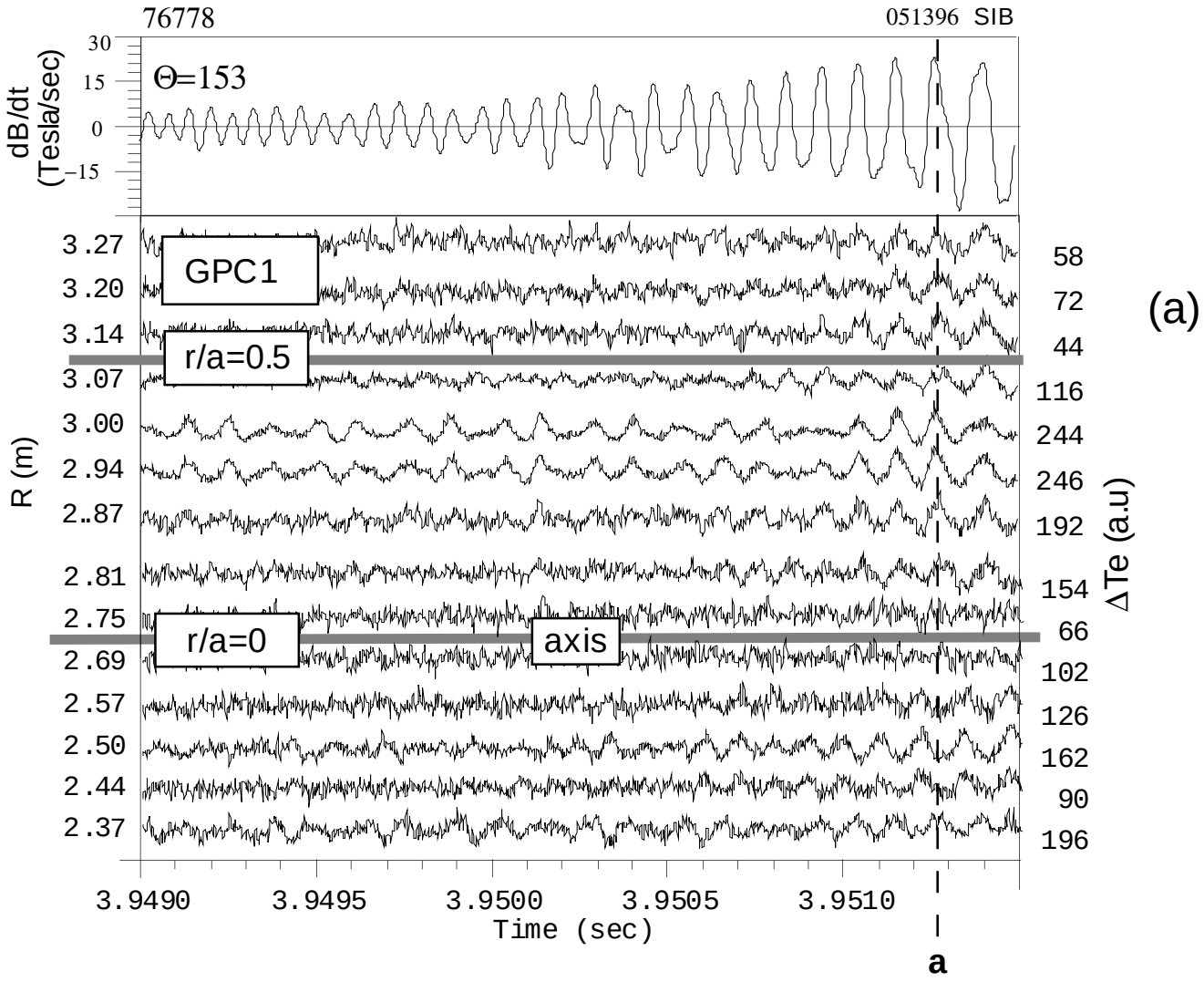
76778
051396 SIB
dB/dt (Tesla/sec)
30
15
0
−15
Θ=153
GPC1
r/a=0.5
r/a=0
axis
R (m)
3.27
3.20
3.14
3.07
3.00
2.94
2.87
2.81
2.75
2.69
2.57
2.50
2.44
2.37
58
72
44
116
244
246
192
154
66
102
126
162
90
196
ΔTe (a.u)
3.9490
3.9495
3.9500
3.9505
3.9510
Time (sec)
a

(a)

Figure 8a

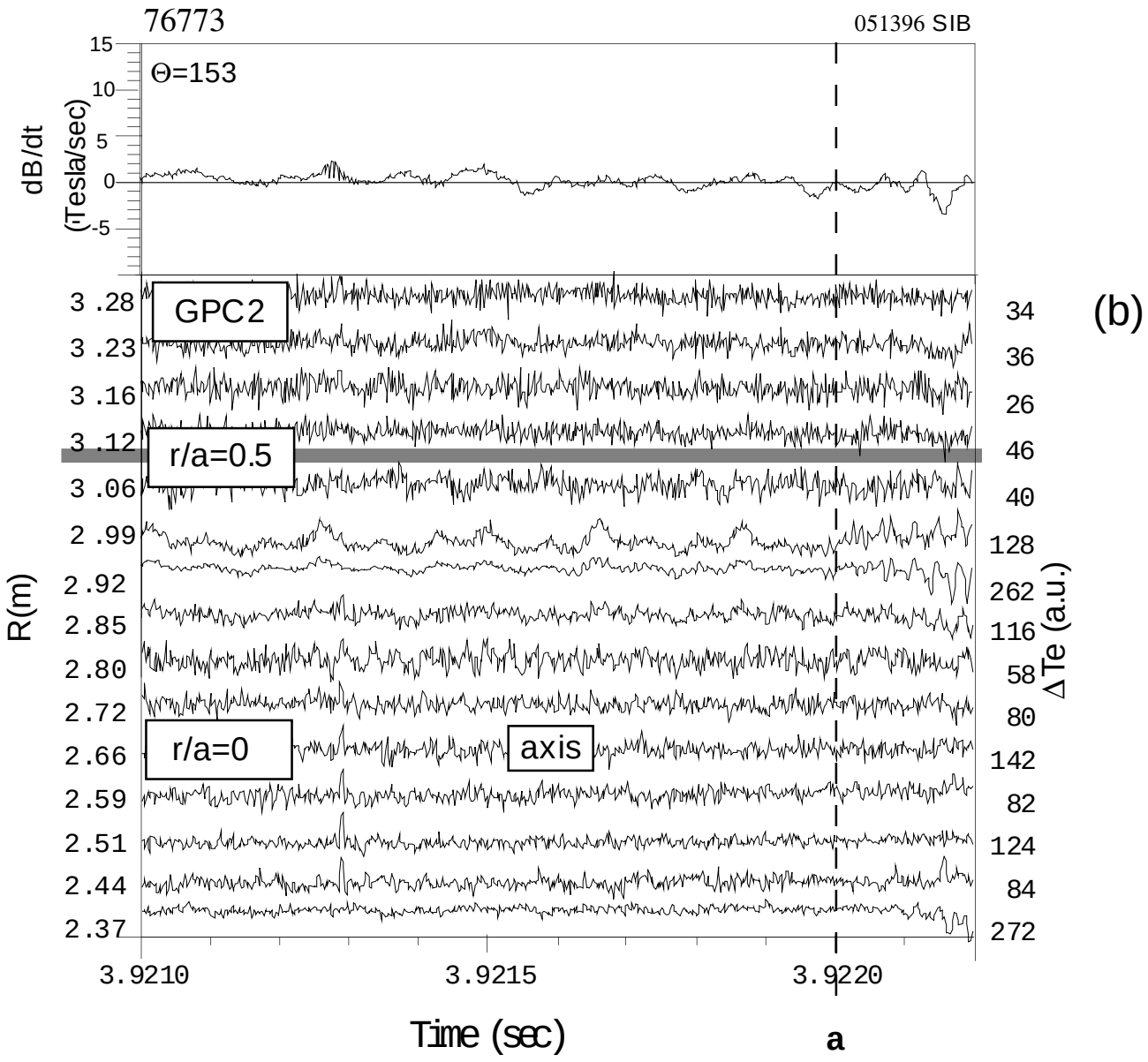
76773
051396 SIB
Θ=153
dB/dt
(Tesla/sec)
15
10
5
0
-5
GPC2
r/a=0.5
r/a=0
axis
R(m)
3.28
3.23
3.16
3.12
3.06
2.99
2.92
2.85
2.80
2.72
2.66
2.59
2.51
2.44
2.37
ΔTe (a.u.)
34
36
26
46
40
128
262
116
58
80
142
82
124
84
272
3.9210
3.9215
3.9220
Time (sec)
a

(b)

Figure 8b

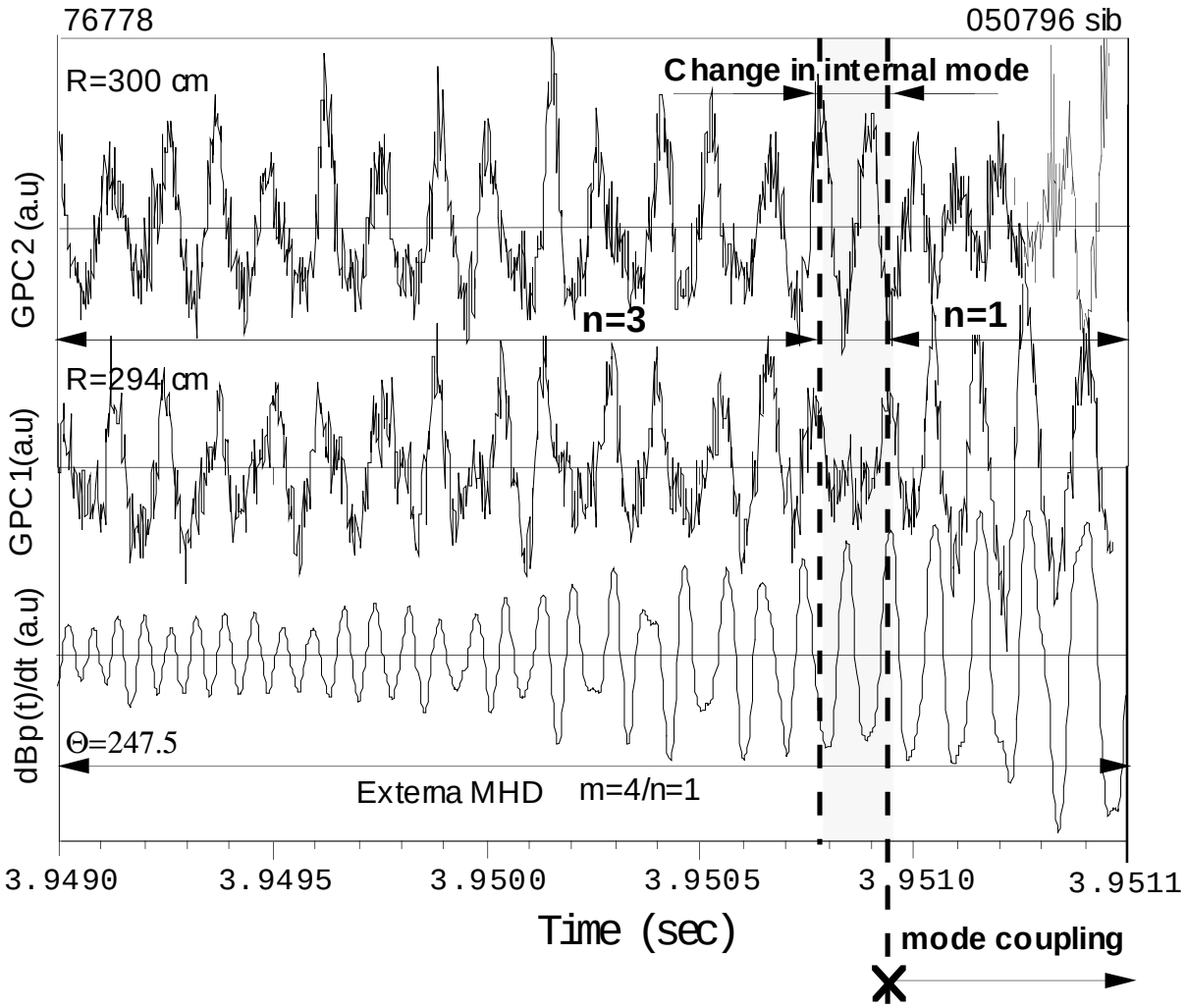
76778
050796 sib
R=300 cm
Change in internal mode
GPC2 (a.u)
n=3
n=1
R=294 cm
GPC1(a.u)
dBp(t)/dt (a.u)
Θ=247.5
Extema MHD m=4/n=1
3.9490
3.9495
3.9500
3.9505
3.9510
3.9511
Time (sec)
mode coupling

Figure 9

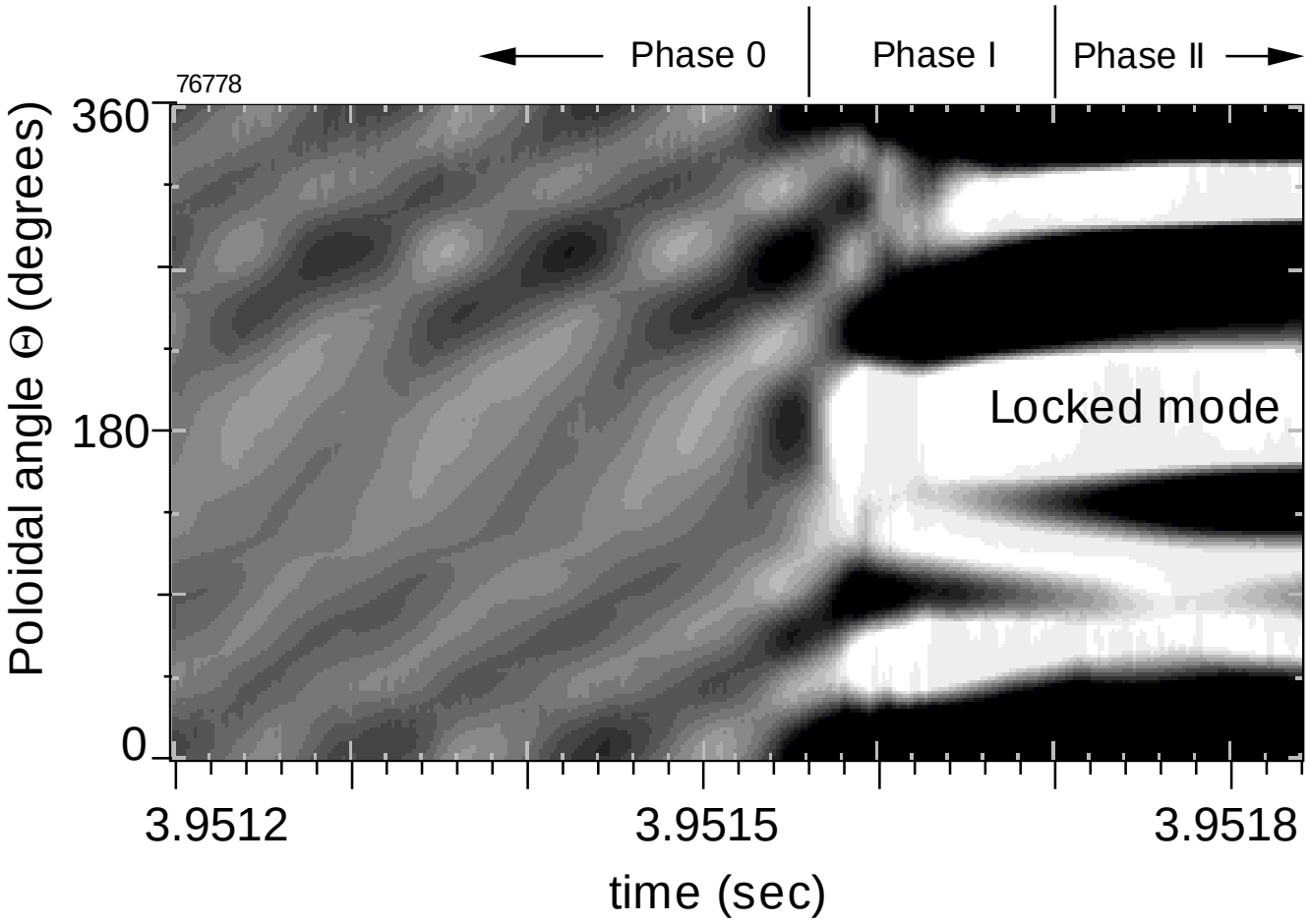
Phase 0
Phase I
Phase II
76778
360
180
0
Poloidal angle Θ (degrees)
Locked mode
3.9512
3.9515
3.9518
time (sec)

Figure 10

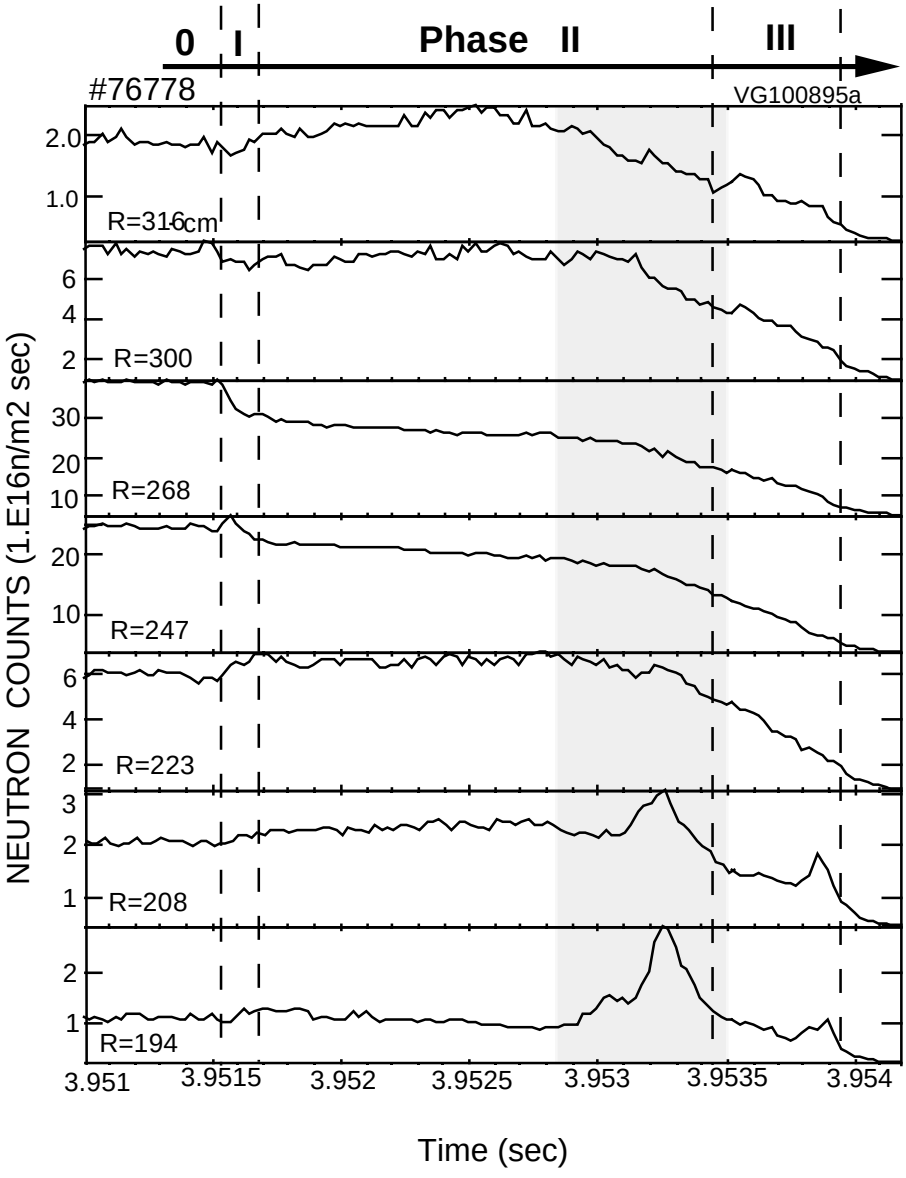
0
I
Phase II
III
#76778
VG100895a
R=316cm
R=300
R=268
R=247
R=223
R=208
R=194
NEUTRON COUNTS (1.E16n/m2 sec)
Time (sec)
3.951
3.9515
3.952
3.9525
3.953
3.9535
3.954

Figure 11